STEM CELLS®

EMBRYONIC STEM CELLS/INDUCED PLURIPOTENT STEM CELLS

Plant Homeo Domain Finger Protein 8 Regulates Mesodermal and Cardiac Differentiation of Embryonic Stem Cells Through Mediating the Histone Demethylation of *pmaip1*

YAN TANG,[a] YA-ZHEN HONG,[a] HUA-JUN BAI,[a] QIANG WU,[a] CHARLIE DEGUI CHEN,[b] JING-YU LANG,[a] KENNETH R. BOHELER,[c] HUANG-TIAN YANG[a,d]

[a]Key Laboratory of Stem Cell Biology, Institute of Health Sciences, Shanghai Institutes for Biological Sciences (SIBS), Chinese Academy of Sciences (CAS) University of Chinese Academy of Sciences & Shanghai Jiao Tong University School of Medicine, Shanghai, China; [b]State Key Laboratory of Molecular Biology, Shanghai Key Laboratory of Molecular Andrology, Institute of Biochemistry and Cell Biology, Shanghai Institutes for Biological Sciences (SIBS), Chinese Academy of Sciences (CAS), Shanghai, China; [c]LKS Faculty of Medicine, Department of Physiology and Stem Cell and Regenerative Medicine Consortium, School of Biomedical Sciences, Jockey Club Building for Interdisciplinary Research, University of Hong Kong, Hong Kong, SAR China; [d]Second Affiliated Hospital, Zhejiang University, Hangzhou, China

Correspondence: Huang-Tian Yang, Ph.D., Institute of Health Sciences, 320 Yue Yang Road, Biological Research Building A, IHS Mail Box 115, Shanghai 200031, China. Telephone: + 86-21-54923280; Fax: + 86-21-54923280; e-mail: htyang@sibs.ac.cn

Received July 25, 2015; accepted for publication January 6, 2016; first published online in STEM CELLS *EXPRESS* February 11, 2016.

1066-5099/2016/$30.00/0

http://dx.doi.org/10.1002/stem.2333

Key Words. Plant homeo domain finger protein 8 • Embryonic stem cells • Mesodermal and cardiac differentiation • Apoptosis • Histone demethylas • Phorbol-12-myristate-13-acetate-induced protein 1

ABSTRACT

Histone demethylases have emerged as key regulators of biological processes. The H3K9me2 demethylase plant homeo domain finger protein 8(PHF8), for example, is involved in neuronal differentiation, but its potential function in the differentiation of embryonic stem cells (ESCs) to cardiomyocytes is poorly understood. Here, we explored the role of PHF8 during mesodermal and cardiac lineage commitment of mouse ESCs (mESCs). Using a *phf8* knockout (*ph8*$^{-/Y}$) model, we found that deletion of *phf8* in ESCs did not affect self-renewal, proliferation or early ectodermal/endodermal differentiation, but it did promote the mesodermal lineage commitment with the enhanced cardiomyocyte differentiation. The effects were accompanied by a reduction in apoptosis through a caspase 3-independent pathway during early ESC differentiation, without significant differences between differentiating wide-type (*ph8*$^{+/Y}$) and *ph8*$^{-/Y}$ ESCs in cell cycle progression or proliferation. Functionally, PHF8 promoted the loss of a repressive mark H3K9me2 from the transcription start site of a proapoptotic gene *pmaip1* and activated its transcription. Furthermore, knockdown of *pmaip1* mimicked the phenotype of *ph8*$^{-/Y}$ by showing the decreased apoptosis during early differentiation of ESCs and promoted mesodermal and cardiac commitment, while overexpression of *pmaip1* or *phf8* rescued the phenotype of *ph8*$^{-/Y}$ ESCs by increasing the apoptosis and weakening the mesodermal and cardiac differentiation. These results reveal that the histone demethylase PHF8 regulates mesodermal lineage and cell fate decisions in differentiating mESCs through epigenetic control of the gene critical to programmed cell death pathways. STEM CELLS *2016;34:1527–1540*

SIGNIFICANCE STATEMENT

Embryonic stem cells (ESCs) have the unique ability to differentiate into derivatives of all three germ layers both in vitro and in vivo. Thus, ESCs provide a unique model for the study of early embryonic development. We report here previously unrecognized effects of histone demethylase plant homeo domain finger protein 8 (PHF8) on mesodermal and early cardiac differentiation. This effect is resulted from the regulation of PHF8 on apoptosis through activating the transcription of pro-apoptotic gene pmaip1. These findings extend the knowledge in understanding of the epigenetic modification in apoptosis during ESC differentiation and of the link between apoptosis and cell lineage decision as well as cardiogenesis.

INTRODUCTION

Embryonic stem cells (ESCs) have the unique ability to differentiate into derivatives of all three germ layers both in vitro and in vivo. Due to this plasticity, mechanisms controlling cell autonomous and regulatory events critical to in vivo mammalian development have benefitted from the in vitro study of differentiating ESCs [1, 2]. Early embryogenesis and cavity formation as well as early ESC differentiation, for example, are accompanied by a reduction in proliferation and increased apoptosis [3–5]. Withdrawal of leukemia inhibitory factor (LIF) from mouse embryonic stem cells (mESCs) cultivated in vitro causes approximately 20%-30% of the cells to die by spontaneous (constitutive) apoptosis [4, 5]. This

occurs secondary to the induction of cleaved caspase 3 [3] and apoptosis-inducing factor (AIF)-complex proteins [6]. Blockade of spontaneous apoptosis in vitro by a p38 mitogen-activated protein kinase (MAPK) inhibitor alters the differentiation markers and increases the abundance of both antiapoptotic proteins (Bcl-2, Bcl-X_L) and Ca^{2+}-binding proteins [4, 7]. In addition, Ca^{2+} released from type 3 inositol 1, 4, 5-trisphosphate receptors (IP_3R3) negatively regulates this apoptotic response, which in turn modulates the mesodermal lineage commitment of early differentiating mESCs [5]. These findings explain, in part, how apoptosis contributes to specific lineage commitment during early development. However, in contrast to the relatively advanced knowledge of signaling pathways [8], little is known about the contribution of epigenetic regulators, especially, histone lysine demethylases (KDMs), in the regulation of apoptosis during ESC differentiation and how the affected programmed cell death by KDMs contributes to the lineage commitment.

Epigenetic regulators and dynamic histone modifications by KDMs are emerging as important players in ESC fate decisions [9]. Histone modifications coordinate transient changes in gene transcription and help maintaining differential patterns of gene expression during differentiation [10–13]. The molecular and biological functions of many KDMs, however, remain enigmatic during ESC differentiation. PHF8, an X-linked gene encoding an evolutionarily conserved histone demethylase harboring an N-terminal plant homeo domain (PHD) and an active jumonji-C domain (JmjC), is able to catalyze demethylation from histones [14, 15]. It is actively recruited to and enriched in the promoters of transcriptionally active genes [14], and it functions to maintain the active state of rRNA through the removal of the repressive H3K9me2 methylation mark at the active rRNA promoters. Mutation of *PHF8* is associated with X-linked mental retardation with cleft lip/cleft palate in human [16–18]. Knockdown of *phf8* in mouse embryonic carcinoma P19 cells impairs neuronal differentiation [19] and leads to brain defects in zebrafish by directly regulating the expression of the homeo domain transcription factor MSX1/MSXB [20]. However, the precise function of PHF8 in the regulation of lineage differentiation derived from other germ layers remains to be identified.

Here, we report previously unrecognized effects of the PHF8 histone demethylase on germ layer commitment and differentiation of mESCs. The results are based on an assessment of early steps of differentiation to mesodermal lineages and cardiomyocytes using *phf8* knockout ($phf8^{-/Y}$) and wild-type ($phf8^{+/Y}$) mESCs. The data show that PHF8 regulates gene transcription of a proapoptotic gene *pmaip1* (also named Noxa) [21]. Activation or repression of *pmaip1* controlled by PHF8 ultimately determines mESC lineage commitment through the regulation of caspase 3-independent apoptosis during mesodermal and cardiac differentiation. Our data reveal that PHF8-mediated the demethylation of histone proteins coordinates ESC lineage commitment through the regulation of apoptosis in early differentiating ESCs.

Materials and Methods

ESC Culture and In Vitro Differentiation

Undifferentiated $Phf8^{+/Y}$ and $Phf8^{-/Y}$ mESCs were maintained on mitomycin C-inactivated mouse embryonic fibroblast (MEF) feeder layers in the presence of LIF (Millipore, Temecula, CA, 1,000 U/ml). The mESC differentiation was performed using a hanging drop method as previously described [5, 22]. Specific ectodermal [23] and endodermal [24] differentiation of mESCs was performed as previously reported.

Generation of *phf8* Knockout mESCs

To generate *Phf8* knockout mESCs, the targeting vector carrying a FRT-flanked neomycin resistant gene and loxP-flanked exons 7 and 8 of *Phf8* as well as an HSV-TK cassette was constructed as shown in Supporting Information Figure S1A. The vector was electroporated into SCR012 mESCs. The mESCs with the FRT sites were selected by G418 followed by Cre mediated recombination of loxP sites to generate the $Phf8^{-/Y}$ mESCs with deleted exons 7 and 8 in the X-chromosome (Supporting Information Fig. S1A).

Generation of *phf8* and *pmaip1* Overexpressing mESC Lines

Full-length mouse *pmaip1* cDNA was generated from mESC RNA by RT-PCR. A cDNA of human *PHF8 (hPHF8)* was amplified from a plasmid encoding *hPHF8* isoform 1 [19]. Both were cloned into the pCDH-EF1-MCS-T2A-Puro lentiviral vectors, respectively (System Biosciences, CA). The viral packaging was performed in 293FT cells after transfection with lipofectamine3000 according to the manufacture's protocol (Invitrogen). A wild-type pCDH-EF1-MCS-T2A-Puro vector was used as a negative control (*NC*). For viral infections, $phf8^{-/Y}$ mESCs were infected with lentiviruses for 6 hours. After 48 hours, infected cells were selected with puromycin for 1 week to generate the stable *pmaip1*-ovexpressing $phf8^{-/Y}$ mESCs ($phf8$-$pmaip1^{-/+}$ mESCs), *hPHF8*-overexpressing $phf8^{-/Y}$ mESCs ($phf8$-$hPHF8^{-/+}$ mESCs), and *NC* $phf8^{-/Y}$ mESCs ($phf8$-$NC^{-/+}$ mESCs). All plasmids were verified by DNA sequencing.

Cell Transfection of Small Interfering RNA

Negative control (si-NC) and *pmaip1* small interfering RNAs (siRNAs) (si-Pmaip1) were synthesized by Gene Pharma (si-NC, 5′-UUCUCCGAACGUGUCACGUTT-3′ and 5′-ACGUG- ACACGUUCGGAGAATT-3′; si-Pmaip1, 5′-GGAUUGGAGACAAAGUGAAT- T-3′ and 5′-UUCACUUUGUCUCCAAUCCTT-3′). si-Pmaip1 and si-NC were transfected into ESCs using DharmaFECT1 (Thermo-fisher, Waltham, MA) according to the manufacturer's instructions.

Immunocytochemical Staining

Undifferentiated mESCs were stained using an ALP substrate kit III (Vector Laboratories, Burlingame, CA) according to the manufacturer's instructions. Immunofluorescence assays were performed as described previously [25]. Briefly, attached cells and embryoid bodies (EBs) were harvested at indicated stages, fixed with 4% paraformaldehyde, permeabilized in 0.3% Triton X-100 (Sigma-Aldrich, St. Louis, MO), blocked in 10% normal goat serum (Vector Laboratories), and then stained with antibodies to stage-specific embryonic antigen 1 (SSEA-1) (Cat No. 13-8813-82, eBioscience, San Diego, CA, 1:200), SRY (sex determining region Y)-box 2 (SOX2) (Cat No. MAB2018, R&D, Minneapolis, MN, 1:200), α-actinin (Cat No. A7732, Sigma-Aldrich, 1:200), cardiac troponin T (TNNT2) (Cat No. ab8295, Abcam, La Jolla, CA, 1:300), or H3K9me2 (Cat No. ab1220, Abcam, 1:200). Antibody labeling was visualized using Alexa Fluor 594 goat anti-mouse IgM (Cat No. A-24921, Invitrogen, Carlsbad, CA, 1:1000),

and DyLight 488- or DyLight 549-conjugated secondary antibodies (all from Jackson Immunoresearch, West Grove, PA, 1:1,000). Nuclei were counterstained with Hoechst 33258 (Sigma-Aldrich, 1:2,000), and cells were analyzed using a Nikon T1 2000 fluorescence microscope. EBs in suspension culture were fixed in 4% paraformaldehyde, embedded in OCT and taken at 20-25 μm thicknesses. The immunostained slices were imaged using a Leica TCS SP2 confocal laser-scanning microscope.

Flow Cytometry Analysis

Tripsinized undifferentiated or differentiating cells were prepared as described [26], and incubated with antibodies to FLK-1 (Cat No. 560070, BD Biosciences, Bedford, MA, 1:200), NESTIN (Cat No. 556309, BD Biosciences, 1:50), SOX17 (Cat No. MAB1924, R&D, 1:25), cardiac troponin T (TNNT2) (Cat No. ab8295, Abcam, 1:200), or α-myosin heavy chain (MYH6) (Cat No. ab50967, Abcam, 1:200). The antibody labeling was visualized using anti-mouse IgG-PE or IgG-PEcy7 (eBioscience, both 1:200). Cells were then analyzed by flow cytometry (FACStar Plus Flow Cytometer, Becton-Dickinson, San Jose, CA).

Cell Viability Assays

A total of 1,000 cells/well were planted in 96-well plates and cultured for 7 days in the presence or absence of LIF and MEF. At indicated times, 10 μl of 5 mg/ml MTT (3-(4,5-dimethylthiazolyl-2)-2,5-diphenyltetrazolium bromide, Sangon Biotech, Shanghai, China) solution was added and incubated for 4 hours. DMSO (Sigma-Aldrich) was then added to solubilize the formazan product and the absorbance was measured at 570 nm.

Cell Proliferation Assays

For bromodeoxyuridine (BrdU) analysis, ESCs were dissociated into single cells and incubated with 100 μM BrdU (Sigma-Aldrich) for 30 minutes. BrdU positive cells were analyzed by flow cytometry (FACStar Plus Flow Cytometer, Becton-Dickinson) using an anti-BrdU APC-conjugated antibody (Cat No. 552598, BD Biosciences, 1:200) according to the manufacturer's instructions.

Cell Cycle Analysis

ESCs were dissociated into single cells, fixed with 70% ethanol and stained with 50 μg/ml propidium iodide (PI) containing 0.1 mg/ml RNase A (both from Sigma-Aldrich). The cells were then analyzed by flow cytometry (FACStar Plus Flow Cytometer, Becton-Dickinson) to detect the cell cycle distribution of G1, S, and G2/M phases.

Apoptosis Assays

Cells were harvested at the indicated times and stained with an Annexin V-FITC Apoptosis Detection Kit (BD Bioscience) to detect early apoptotic cells according to the manufacturer's instructions. Terminal deoxynucleotidyl-transferase-mediated dUTP-biotin nick end labeling (TUNEL) assay was used to monitor late stage apoptosis with the in situ Cell Death Detection Kit (Roche, Mannheim, Germany), according to the manufacturer's instructions. Annexin V signal and TUNEL signal were detected by flow cytometry (FACStar Plus Flow Cytometer, Becton-Dickinson). DNA Laddering assay was performed using the Apoptotic DNA Ladder Kit (Applygen, Beijing, China) and analyzed on 1.5% agarose gels.

RNA Extraction, Reverse Transcription-PCR and Quantitative RT-PCR

Total RNA was isolated using Trizol (Invitrogen) and analyzed by reverse transcription-PCR (RT-PCR) and quantitative RT-PCR (qRT-PCR) as described [26]. The transcripts of *m28s* and *gapdh* were used for internal controls. The RT-PCR primers are listed in Supporting Information Table S1, and the qRT-PCR primers are listed in Supporting Information Table S2.

Western Blot Assay

Experiments were performed as described [5]. Briefly, cells were lysed in a lysis buffer and 30 μg of protein extract supernatant was used for Western blots. Blots were incubated with the primary antibody against H3K9me2 (Cat No. ab1220, Abcam, 1:1,000), PHF8 (Cat No. ab36068, Abcam, 1:500), β-actin (Cat No. BM0627, Boster, Wuhan, China, 1:4,000), caspase 3 (Cat No. 9662, Cell Signaling Technology, Beverly, MA, 1:500), H3 histone (Cat No. 4620, Cell Signaling Technology, 1:2,000), or Poly (ADP-ribose) polymerase 1 (PARP1) (Cat No. 9542, Cell Signaling Technology, 1:1,000). The membranes were then incubated with IRDye 680LT Donkey anti-Rabbit IgG (Cat No. 926-68023, Li-COR Biosciences, Lincoln, NE) or IRDye 800LT Donkey anti-Mouse IgG (Cat No. 926-32212, Li-COR Biosciences) as secondary antibodies and visualized on an Odyssey Infrared Imager (Li-COR Biosciences).

mRNA Microarray Analysis

Three replicates from either *phf8*$^{+/Y}$ or *phf8*$^{-/Y}$ ESCs were used for RNA extraction. Quality-assessed RNA samples were supplied for a whole mouse gene expression microarray using GeneChip Mouse Genome 430 2.0 (Affymetrix, Santa Clara, CA). Eighteen raw data files generated by the Affymetrix scanner passed data quality control were further performed with RMA normalization through the Affymetrix expression console. Further analysis was performed using SAM (significance analysis of microarrays) software [27], and the hierarchical average linkage clustering was performed using Cluster version 3.

Chromatin Immunoprecipitation Assay

Chromatin immunoprecipitation (ChIP) experiments were performed using a Simple ChIP™ Enzymatic Chromatin IP Kit (Cell Signaling Technology) according to the manufacturer's instructions. Protein-DNA complexes were immunoprecipitated with antibodies against PHF8 (Cat No. ab36068, Abcam), H3K9me2 (Cat No. ab1220, Abcam), and normal rabbit IgG (Cat No. 2729, Cell Signaling Technology). The purified DNA was quantified by qRT-PCR with SYBR Green PCR reagents (Toyobo, Osaka, Japan) to detect the enrichment of *pmaip1* with the specific primers 5′-GTCCCGATAAAATGCGAGAG-3′ (forward) and 5′-GGGAGACTA-AGGTCCCCAAT-3′ (reverse), and normalized to the total input control.

Statistical Analysis

Data analysis was performed using Microsoft GraphPad Prism 5 (GraphPad Software, LA Jolla, CA). The data were shown as mean + SEM. The statistical significance of differences was estimated by ANOVA or Student's *t* test as appropriate. $p < .05$ was considered to be statistically significant.

Results

Deletion of *phf8* Promotes Mesodermal and Cardiac Lineage Commitment

The PHF8 protein was detectable in undifferentiated ESCs, but its abundance significantly increased within one day of LIF withdrawal. Then it gradually decreased to a level at day 5 lower than that observed in the undifferentiated ESCs (Fig. 1A).

To determine the significance of *phf8* gene expression on ESC fate decision, we knocked out the X-chromosome-encoded *phf8* gene in one allele of male SCR012 ESCs by deletion of exons 7 and 8 through Cre-mediated recombination (Supporting Information Fig. S1A). Gene inactivation was confirmed by the lack of Phf8 mRNA and PHF8 protein expression in these targeted ESCs (Supporting Information Fig. S1B). Transcripts for pluripotency marker genes *nanog, rex1* (*zfp42*), *sox2*, and *oct4* (*pou5f1*) were not significantly different between $phf8^{+/Y}$ and $phf8^{-/Y}$ ESCs (Fig. 1B). No significant difference was observed in cell morphology (Supporting Information Fig. S1C) of undifferentiated $phf8^{+/Y}$ and $phf8^{-/Y}$ ESCs or in alkaline phosphatase activity (Supporting Information Fig. S1D). Immunofluorescence staining confirmed that the expression of pluripotency marker SOX2 and SSEA-1 did not differ between the $phf8^{+/Y}$ and $phf8^{-/Y}$ ESCs (Supporting Information Fig. S1E). These results indicate that *phf8* may be dispensable for normal growth and maintenance of mESCs.

We then analyzed the role of PHF8 in the mesodermal and cardiac lineage commitment. By microarray analysis of differentiating $phf8^{+/Y}$ and $phf8^{-/Y}$ cells from days 0, 1, to 3.5, we found a significant decrease in transcripts for pluripotency markers, accompanied by a significant increase in transcripts for ectoderm, mesoderm and endoderm, while in $phf8^{-/Y}$ cells some transcripts for mesodermal and cardiac lineage commitment were significantly enhanced compared with those in $phf8^{+/Y}$ cells (Supporting Information Fig. S2A). These differentiation-dependent changes in transcript abundance were confirmed by qRT-PCR for early mesodermal markers brachyury (*T*) [28], goosecoid (*gsc*), *eomes* [29], and *mesp1* [30], cardiovascular progenitor marker *flk-1* [31, 32] and neuropilin 1 (*nrp1*) [33]. Early cardiac transcription factors, including myocyte enhancer factor 2C (*mef2c*) [34], *hand1* [35], and *tbx5* [36, 37] were also up-regulated in $phf8^{-/Y}$ cells at differentiation day 5, while no difference in the expression levels of pluripotent markers *oct4* (Fig. 1C), *rex1*, and *nanog* (Supporting Information Fig. S2B) were detected between $phf8^{+/Y}$ and $phf8^{-/Y}$ cells at the time points examined.

Because mESCs can differentiate into all three germ layers, we also examined whether *phf8* affected ectodermal and endodermal differentiation. qRT-PCR analysis did not show any significantly difference in the expression of early ectodermal markers *nestin* and *fgf5* between the $phf8^{+/Y}$ and $phf8^{-/Y}$ cells (Fig. 1D). Moreover, in the induced early ectodermal differentiation system [23], the expression of ectodermal markers *nestin, fgf5*, and *pax6* were comparable between the $phf8^{+/Y}$ and $phf8^{-/Y}$ cells (Supporting Information Fig. S3A). Besides, the expression of endodermal markers *afp, foxa2, sox17*, and *gata4* were not significantly different between the $phf8^{+/Y}$ and $phf8^{-/Y}$ cells (Fig. 1E). Consistently, the expression of endodermal markers *foxa2, sox17*, and *gata4* were comparable during induced endodermal differentiation [24] between the $phf8^{+/Y}$ and $phf8^{-/Y}$ cells (Supporting Information Fig. S3B). Thus, *phf8* appears not to affect early ectodermal and endodermal differentiation.

The increased mesodermal and cardiac marker expressions were associated with a significant increase in the total number of cardiac progenitors and cardiomyocytes in differentiating $phf8^{-/Y}$ cells. By flow cytometry analysis, marked increases in the population of FLK-1 positive ($FLK\text{-}1^{+}$) cells were detected in $phf8^{-/Y}$ cells at differentiation day 3 and day 4 (Fig. 2A). Consistently, the percentage of contracting EBs was higher in $phf8^{-/Y}$ cells than in $phf8^{+/Y}$ cells (Fig. 2B). The transcripts for progenitor marker *nrp1*, early cardiac transcription factor *tbx5*, and cardiac specific genes *tnnt2, myh6, myl2*, and *gja1* were higher in $phf8^{-/Y}$ EBs than those in $phf8^{+/Y}$ ones (Fig. 2C). The areas of immunostained EBs positive for the cardiac cytoskeletal and myofilamental proteins α-actinin and TNNT2 were also greater in $phf8^{-/Y}$ than in $phf8^{+/Y}$ EBs (Fig. 2D). Flow cytometry analysis of $MYH6^{+}$ (Fig. 2E) and $TNNT2^{+}$ (Fig. 2F) cells at differentiation day 9 further confirmed the increase of cardiomyocytes in $phf8^{-/Y}$ cells. Taken together, these data indicate that the *phf8* deletion facilitates the differentiation of mesodermal and cardiac linage commitment.

PHF8 Inactivation Increases Cell Viability but not Proliferation of the Differentiating ESCs

Differentiation of both $phf8^{+/Y}$ and $phf8^{-/Y}$ ESCs via EB formation produced normal round shaped EBs but, by day 3, $phf8^{-/Y}$ EBs were larger than those generated from $phf8^{+/Y}$ ESCs, and the size differences were visibly obvious at differentiation days 5 and 7 (Fig. 3A). Although no significant differences in cell viability could be demonstrated between undifferentiated $phf8^{+/Y}$ and $phf8^{-/Y}$ ESCs (Fig. 3B), the viability of $phf8^{-/Y}$ cells was significantly greater than that in $phf8^{+/Y}$ cells at differentiation days 3 to 7 (Fig. 3C). However, no significant change in BrdU staining was detected by flow cytometry between $phf8^{+/Y}$ and $phf8^{-/Y}$ ESCs at differentiation days 0, 3, or 5 (Fig. 3D). Moreover, no significant difference in the cell cycle distribution between the differentiating $Phf8^{+/Y}$ and $Phf8^{-/Y}$ ESCs was detected, although the percentage of cells in S phase gradually decreased while those in G1 phase increased upon differentiation (Fig. 3E). Knockout of *phf8* thus increases cell numbers in the early differentiating ESCs through the improvement of cell viability without changes in cell proliferation or cell cycle progression.

PHF8 Regulates Apoptosis During the Early Stage of Cardiac Lineage Commitment

We then examined whether cell death might account for the differences in the cell viability observed between the differentiating $phf8^{+/Y}$ and $phf8^{-/Y}$ ESCs. In undifferentiated ESCs, no significant difference was demonstrated with Annexin V (an early apoptosis marker) staining, TUNEL assay, total DNA fragmentation or caspase 3 protein cleavage between $phf8^{+/Y}$ and $phf8^{-/Y}$ cells (Fig. 4A--4C, 4E). In contrast, Annexin V staining (Fig. 4A) and TUNEL assay (Fig. 4B) showed significant decreases in the number of apoptotic cells in $phf8^{-/Y}$ ESCs at differentiation days 3 and 5 compared with those in $phf8^{+/Y}$ cells. Genomic DNA fragmentation with a pattern typical for apoptosis was detected in $phf8^{+/Y}$ cells at differentiation days 3 and 5, but it was reduced in $phf8^{-/Y}$ cells at the same time

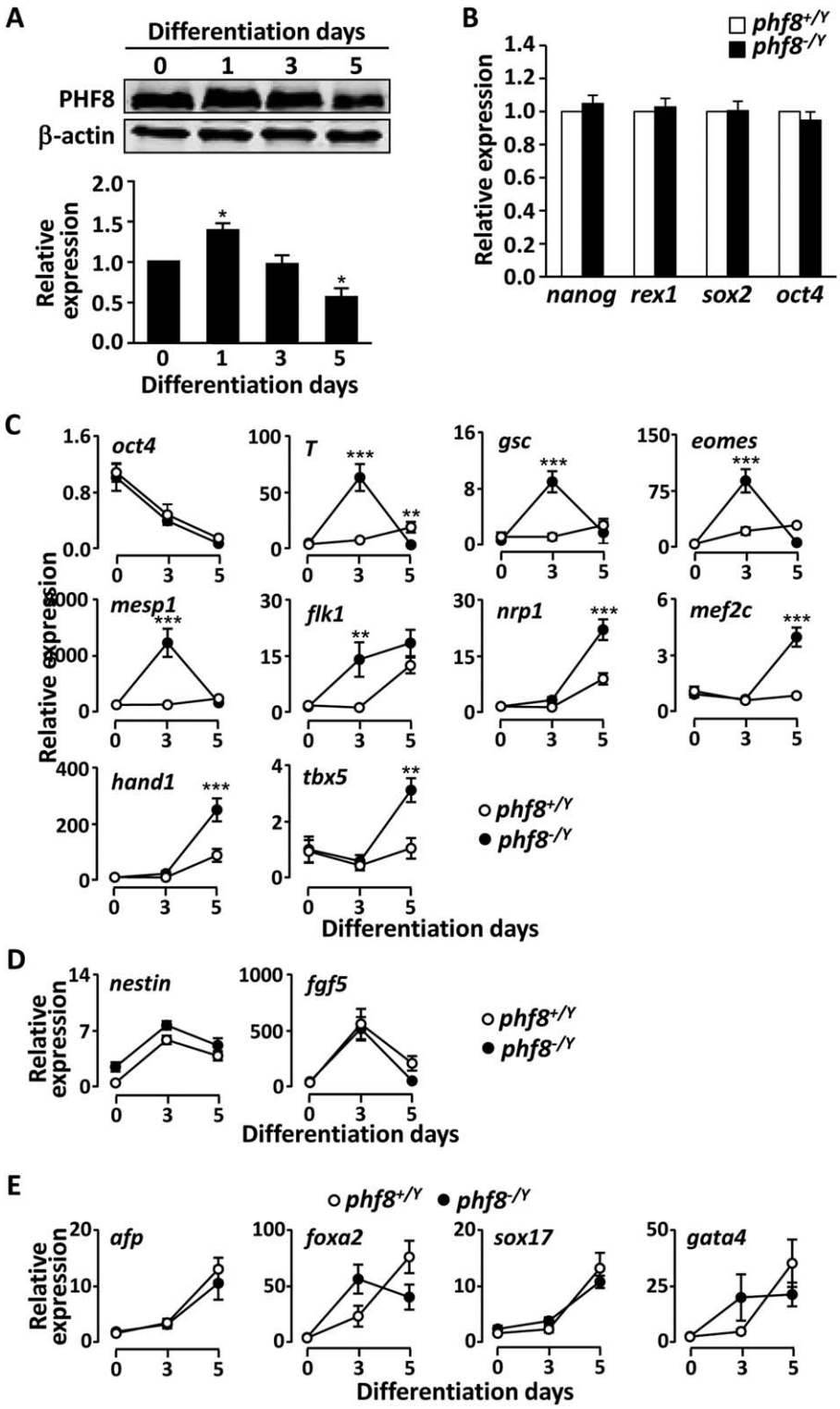

Figure 1. Plant homeo domain finger protein 8 (PHF8) regulates the mesodermal and early cardiac differentiation of mouse embryonic stem cells (mESCs). (**A**): Western blot analysis of PHF8 expression in undifferentiated and differentiating ESCs. $n = 3$. (**B**): quantitative RT-PCR (qRT-PCR) analysis of pluripotency markers *nanog, rex1, sox2*, and *oct4.* $n = 8$. (**C**): qRT-PCR analysis of gene expression of pluripotency marker *oct4*; early mesodermal markers brachyury (*T*), *gsc, eomes*, and *mesp1*; cardiovascular progenitor markers *flk-1* and *nrp1*; and the cardiac transcription factors *hand1, tbx5*, and *mef2c* during ESC differentiation. $n = 5$. (**D**): qRT-PCR analysis of the early ectodermal markers *nestin* and *fgf5* during ESC differentiation. $n = 3$. (**E**): qRT-PCR analysis of early endodermal markers *afp, foxa2, sox17*, and *gata4* during ESC differentiation. $n = 3$. Data are presented as mean ± SEM *, $p < .05$; **, $p < .01$; ***, $p < .001$ compared with the corresponding $phf8^{+/Y}$ value.

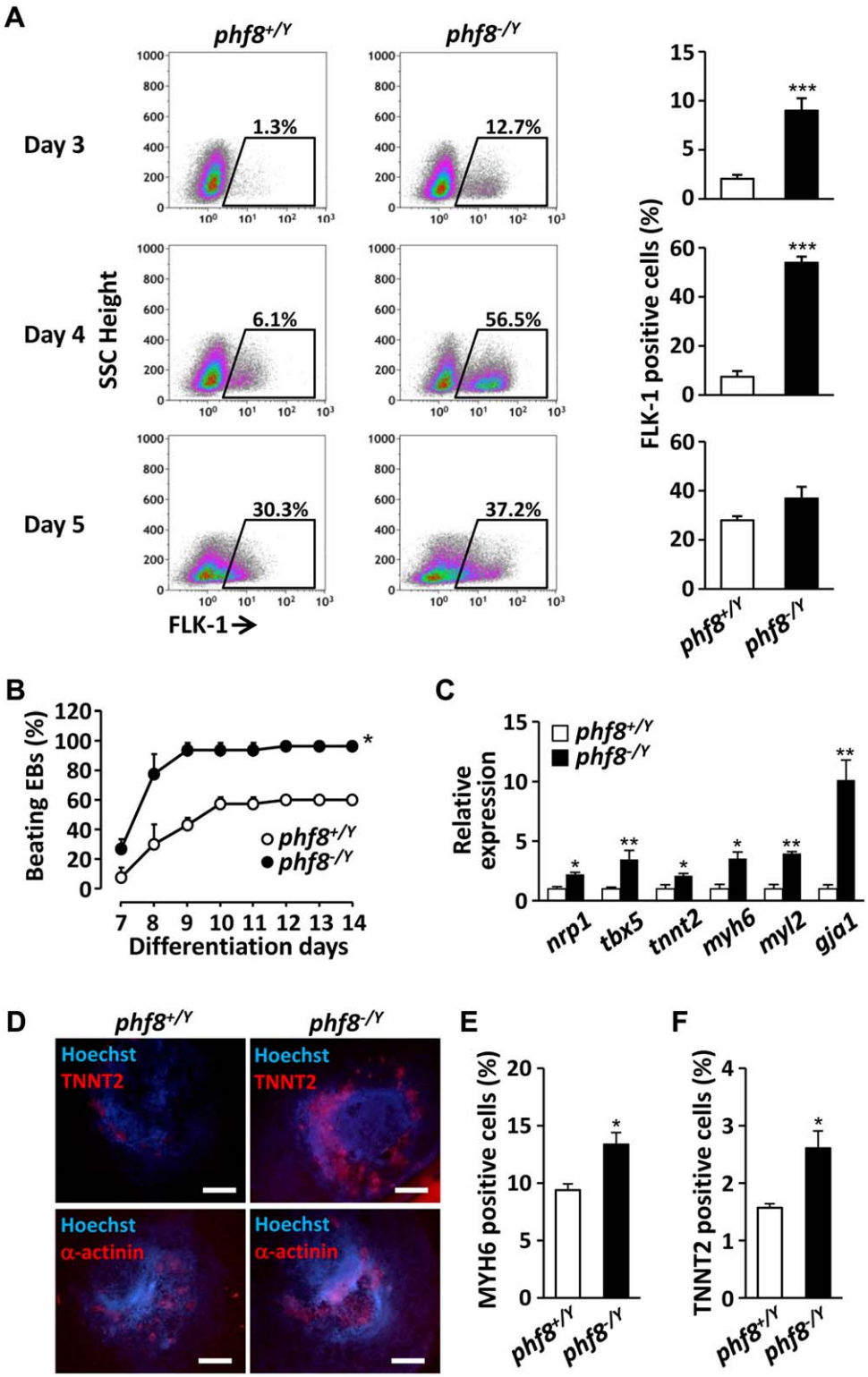

Figure 2. *phf8* deletion promotes cardiac differentiation of mouse embryonic stem cells (mESCs). (**A**): Left, representative flow cytometry plots showing FLK-1 expression at differentiation day 3 ($n = 6$), day 4 and day 5 ($n = 3$ each). Right, the quantification of flow cytometry data. (**B**): Differentiation profile of cardiomyocytes during embryoid bodies (EB) outgrowth. $n = 6$. (**C**): qRT-PCR analysis of ESCs for the expression of cardiac markers at differentiation day 14. $n = 3$. (**D**): Immunofluorescence analysis of TNNT2 and α-actinin in day 14 EBs. Scale bars = 400 μm. (**E**) Flow cytometry analysis of MYH6 positive cells and (**F**) TNNT2 positive cells in day 9 EBs. $n = 3$ each. Data are presented as mean ± SEM *, $p < .05$; **, $p < .01$; ***, $p < .001$ compared with the corresponding $phf8^{+/Y}$ value.

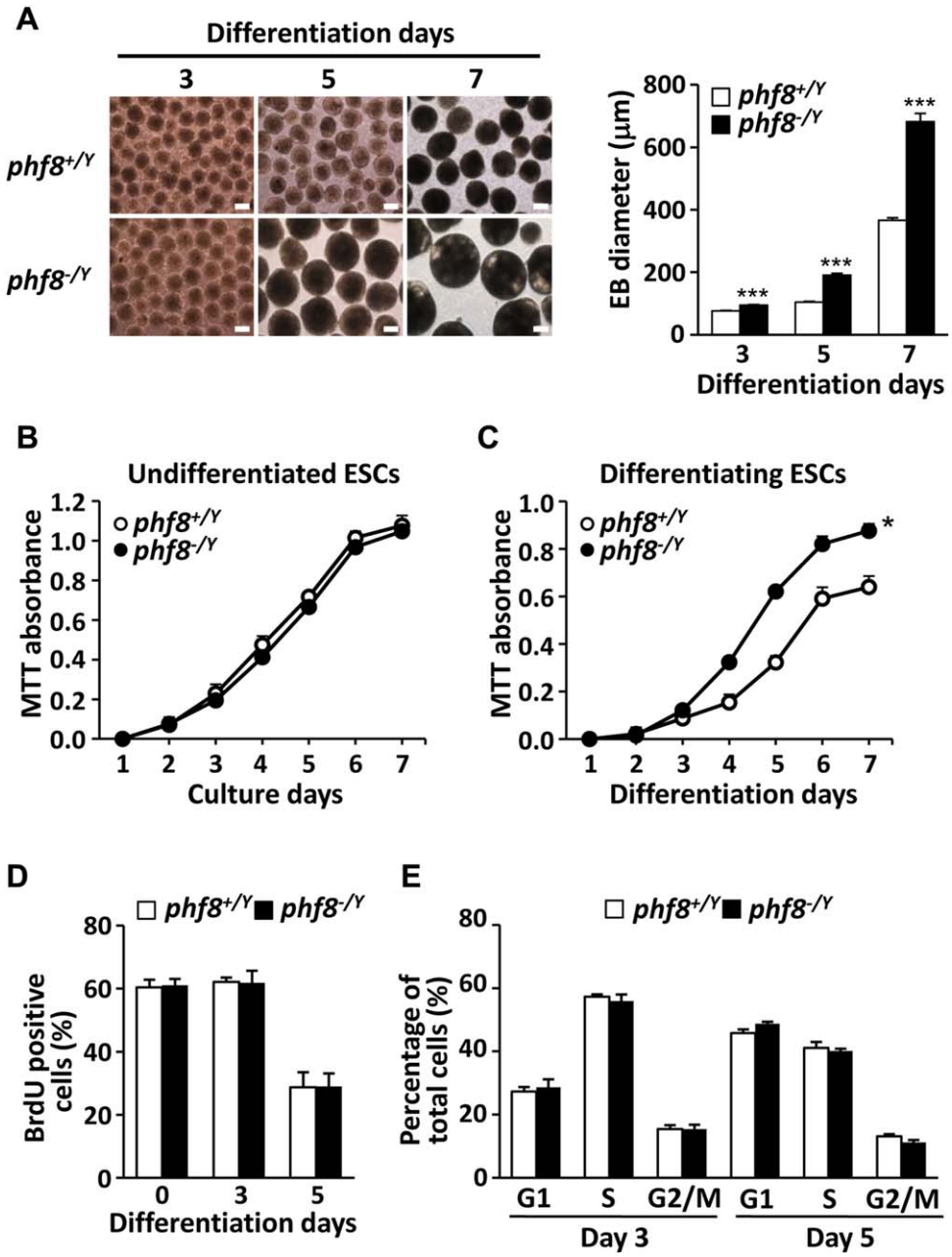

Figure 3. *phf8* deletion increases cell viability in differentiating mouse embryonic stem cells (mESCs) without affecting cell proliferation. (**A**): Left, phase-contrast images of embryoid bodies (EB) morphology during EB formation from ESCs. Scale bar = 200 μm. Right, the diameter of EB formed from ESCs. (**B**): Cell viability of undifferentiated and (**C**): differentiating ESCs analyzed by MTT assay for seven consecutive days. $n = 3$. (**D**): Flow cytometry analysis of BrdU positive proportion of undifferentiated ($n = 4$) and differentiating ESCs at day 3 and day 5. $n = 5$ each. (**E**): Flow cytometry analysis of cell cycle distribution by propidium iodide (PI) staining at differentiation day 3 ($n = 6$) and day 5 ($n = 3$). Data are presented as mean ± SEM *, $p < .05$; ***, $p < .001$ compared with the corresponding $phf8^{+/Y}$ value.

points (Fig. 4C). Moreover, approximately 35% of Annexin V^+ cells were present in FLK-1^+/$phf8^{+/Y}$ cells at differentiation day 4, whereas only 9% of the cells were Annexin V^+ in FLK-1^+/$phf8^{-/Y}$ cells (Fig. 4D). The ratio of $TUNEL^+$ to either $NESTIN^+$ (ectoderm) or $SOX17^+$ (endoderm) cells did not differ between the $phf8^{+/Y}$ and $phf8^{-/Y}$ cells (Supporting Information Fig. S3C, S3D). In addition, $phf8^{+/Y}$ ESCs at differentiation days 3 and 5 increased the caspase 3 cleavage (Fig. 4E, upper and lower left panels) and the ratio of cleaved caspase 3 to total caspase 3 protein (Fig. 4E, lower right panel). Unexpectedly, the ratio of cleaved caspase 3 to total caspase 3 in $phf8^{-/Y}$ ESCs did not significantly differ from that observed in $phf8^{+/Y}$ ones. Consistently, a significant enhancement of the downstream target PARP1 cleavage [38, 39] was observed at differentiation days 3 and 5, but it was comparable between the $phf8^{+/Y}$ and $phf8^{-/Y}$ cells (Fig. 4F). These data suggest that the cell death associated with *phf8* function does not operate through the conventional caspase 3-mediated apoptosis.

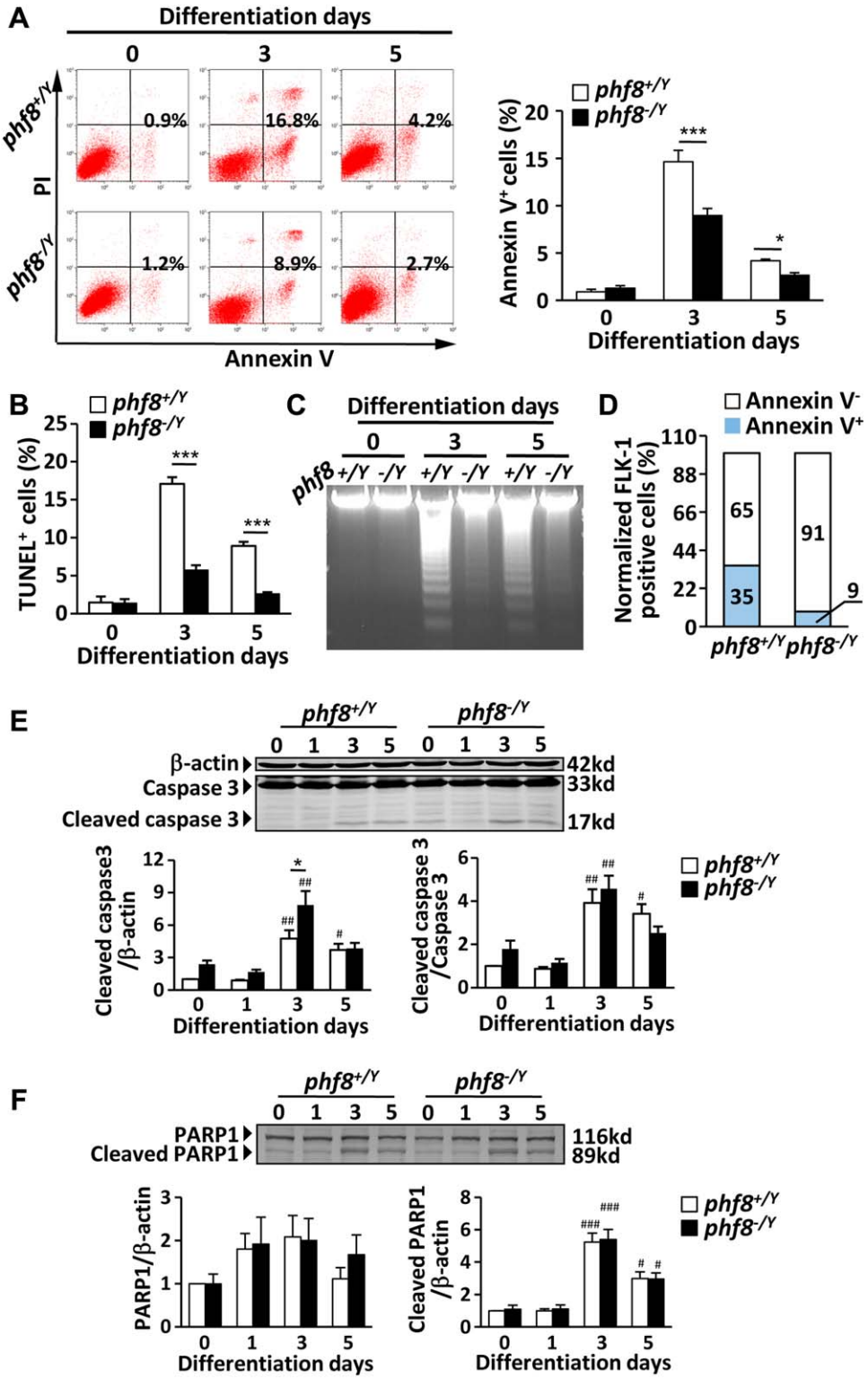

Figure 4. Plant homeo domain finger protein 8 (PHF8) regulates apoptosis during the early mouse embryonic stem cells (mESC) differentiation. (**A**): Left, representative flow cytometry plots showing Annexin V (*x*-axis), and PI (*y*-axis) staining in ECSs at differentiation day 0 ($n = 4$), day 3 ($n = 3$) and day 5 ($n = 7$). Right, the quantification of flow cytometry data. (**B**): Flow cytometry detection of apoptotic responses of TUNEL positive cells at differentiation day 0 ($n = 3$), day 3 ($n = 4$), and day 5 ($n = 4$). (**C**): DNA laddering analysis at differentiation days 0, 3, and 5. $n = 6$ each. (**D**): Cells double stained with FLK-1 and Annexin V were analyzed by flow cytometry at differentiation day 4. $n = 3$. (**E**): Western blot analysis of caspase 3 during the mESC differentiation. β-actin was used as a loading control. $n = 4$. (**F**): Western blot analysis of PARP1 expression during the differentiation. β-actin was used as a loading control. $n = 4$. Data are presented as mean ± SEM *, $p < .05$; ***, $p < .001$ compared with the corresponding $phf8^{+/Y}$ value; $^{\#}$, $p < .05$; $^{\#\#}$, $p < .01$ compared with the corresponding d0 value.

pmaip1 is a Direct Target Gene of PHF8 in the Early Differentiating ESCs

To understand how PHF8 might regulate apoptosis during early ESC differentiation, we compared the profiles of apoptosis-related gene transcripts in undifferentiated and early differentiating *phf8*$^{+/Y}$ and *phf8*$^{-/Y}$ ESCs using gene expression microarrays. Among the apoptosis-related genes, the transcript to *pmaip1*, a proapoptotic Bcl-2 family member crucial in fine-turning the cell death decision [21, 40–42], was markedly increased during early differentiation of *phf8*$^{+/Y}$ cells but it was reduced in *phf8*$^{-/Y}$ cells at differentiation days 1 and 3.5 (Fig. 5A). These expression patterns were confirmed by qRT-PCR during cardiac differentiation (Fig. 5B), and the results were consistent with the apoptotic pattern observed during the early ESC differentiation (Fig. 4A--4C). In addition, qRT-PCR analysis showed that the expression of *pmaip1* did not show any significant difference between the *phf8*$^{+/Y}$ and *phf8*$^{-/Y}$ cells during the induced ectodermal (Supporting Information Fig. S3E) or endodermal (Supporting Information Fig. S3F) differentiation.

A direct link between the PHF8 and *pmaip1* was then confirmed by ChIP analysis. We detected the endogenous binding of PHF8 at the transcription start site (TSS, from −45 bp to 104 bp) of *pmaip1* in *phf8*$^{+/Y}$ ESCs and determined that binding was enhanced at differentiation day 3. The binding of PHF8 was not detectable above the IgG control levels in *phf8*$^{-/Y}$ cells (Fig. 5C). Global methylation (H3K9me2 normalized to H3) was unchanged at differentiation days 3 and 5, but it was significantly enhanced at differentiation day 1 in *phf8*$^{-/Y}$ cells (Fig. 5D). The augmentation of H3K9me2 methylation in *phf8*$^{-/Y}$ ESCs was then confirmed by immunostaining at differentiation day 1 (Fig. 5E). An increase in the repressive mark of H3K9me2 was also observed at the TSS of *pmaip1* in the early differentiating *phf8*$^{-/Y}$ ESCs (Fig. 5F), indicating that the PHF8 demethylase activity is actively involved in the regulation of *pmaip1* gene.

Transient Knockdown of *pmaip1* Decreases Apoptosis and Promotes Mesodermal and Cardiac Differentiation

To clarify the role of *pmaip1* in mESC differentiation, we transfected specific siRNAs against *pmaip1* (si-Pmaip1) into *phf8*$^{+/Y}$ ESCs followed by EB formation. The negative control siRNA (si-NC) did not alter *pmaip1* transcript levels compared with untreated (NT) cells, while si-Pmaip1 significantly inhibited *pmaip1* transcripts by 74%-76% at differentiation days 0 and 1 (Fig. 6A-a). si-Pmaip1 cells had fewer TUNEL^{+} cells compared with the NT and si-NC cells at differentiation day 3 in both *phf8*$^{+/Y}$ and *phf8*$^{-/Y}$ cells (Fig. 6A-b). We then examined whether the *pmaip1* knockdown influences mesodermal and early cardiac differentiation. As shown in Figure 6B, the apoptosis of FLK-1^{+} cells was significantly decreased in si-Pmaip1 mESCs (Fig. 6B). The expression of *T* and *gsc* as well as *nrp1* and *flk-1* were increased in si-Pmaip1 cells compared with those in NT and si-NC cells at differentiation day 3. In addition, the expression of cardiac transcript factors *mef2c* and *tbx5* was upregulated at differentiation day 5, and *myh6* and *tnnt2* were upregulated at differentiation day 9 (Fig. 6C). We also transfected si-Pmaip1 into *phf8*$^{-/Y}$ ESCs. The expression of *pmaip1* was downregulated at differentiation day 0 and day 1 in *phf8*$^{-/Y}$ ESCs with si-Pmaip1 (Supporting Information as Fig. S4A-a), accompanied by a decrease in TUNEL^{+} cells compared with NT and si-NC (Fig. 6A-b), while Annexin V remained unchanged (Supporting Information Fig. S4A-b). The expression of *nrp1* and *flk1* did not significantly change in *phf8*$^{-/Y}$ ESCs with si-Pmaip1 at differentiation day 3, while *mef2c* was upregulated at differentiation day 5, and *myh6* was upregulated at differentiation day 9 (Supporting Information as Fig. S4B). These results suggest that downregulation of *pmaip1* in *phf8*$^{-/Y}$ ESCs may not lead to as robust of a phenotype as it did in *phf8*$^{+/Y}$ ESCs. This difference is likely due to the level of *pmaip1* during early differentiation of *phf8*$^{-/Y}$ ESCs was already decreased to a low level similar to that observed in the undifferentiated cells (Fig. 5B). Taken together, these data demonstrate that the decreased apoptosis via down-regulation of *pmaip1* contributes, at least partially, to the *phf8*$^{-/Y}$-facilitated mesodermal and cardiomyocyte commitment.

Overexpression of *pmaip1* or *hPHF8* in *phf8*$^{-/Y}$ ESCs Increases Apoptosis and Weakens Mesodermal and Cardiac Differentiation

To further determine whether PHF8 contributes to mesoderm and cardiac cell commitment through the regulation of apoptosis via targeting *pmaip1*, we rescued the expression of *pmaip1* and *phf8* in *phf8*$^{-/Y}$ ESCs by generating *pmaip1*-ovexpressing *phf8*$^{-/Y}$ mESCs (*phf8-pmaip1*$^{-/+}$ mESCs) and *hPHF8*-overexpressing *phf8*$^{-/Y}$ mESCs (*phf8-hPHF8*$^{-/+}$ mESCs). The qRT-PCR analysis confirmed that the expression of *hPHF8* or *pmaip1* was significantly upregulated in the respective overexpressing cell lines (Supporting Information Fig. S4C). The expression of *pmaip1* in undifferentiated *phf8*$^{-/Y}$ mESCs was not affected by *hPHF8* overexpression. However, Pmaip1 transcripts increased by differentiation day 3 in overexpressing cells (Supporting Information Fig. S4D), indicating that PHF8 does regulate the expression of *pmaip1* during differentiation. Both TUNEL and Annexin V analysis revealed significant increases of apoptosis in *phf8-pmaip1*$^{-/+}$ and *phf8-hPHF8*$^{-/+}$ mESCs compared with the *phf8*$^{-/Y}$ and *phf8-NC*$^{-/+}$ mESCs at differentiation day 3 or day 4, accompanied by a higher apoptosis ratio in FLK-1^{+} cells (Fig. 6D). Moreover, the expression of *T* and *gsc* as well as *nrp1* and *flk-1* were significantly decreased in *phf8-pmaip1*$^{-/+}$ and *phf8-hPHF8*$^{-/+}$ mESCs at differentiation day 3, followed by a down-regulation of *mef2c* and *tbx5* at differentiation day 5, and *myh6* and *tnnt2* at differentiation day 9 (Fig. 6E). In addition, TUNEL analysis showed no changes in the apoptotic responses either through knockout or overexpression of *phf8* compared with the corresponding wild-type cells or *phf8*$^{+/Y}$ cells during induced ectodermal differentiation (Supporting information Fig. S4E). These data are consistent with a regulatory role of *phf8* on mesodermal and cardiac differentiation through targeting of *pmaip1*.

Discussion

This is the first study to unravel a regulatory role of histone demethylase in the differentiation of ESCs through the control of apoptosis and subsequent effects on cell lineage commitment. The role of PHF8 in the regulation of ESC differentiation to the mesodermal lineage and cardiac differentiation is supported by selective changes in RNA markers for mesodermal lineages, and

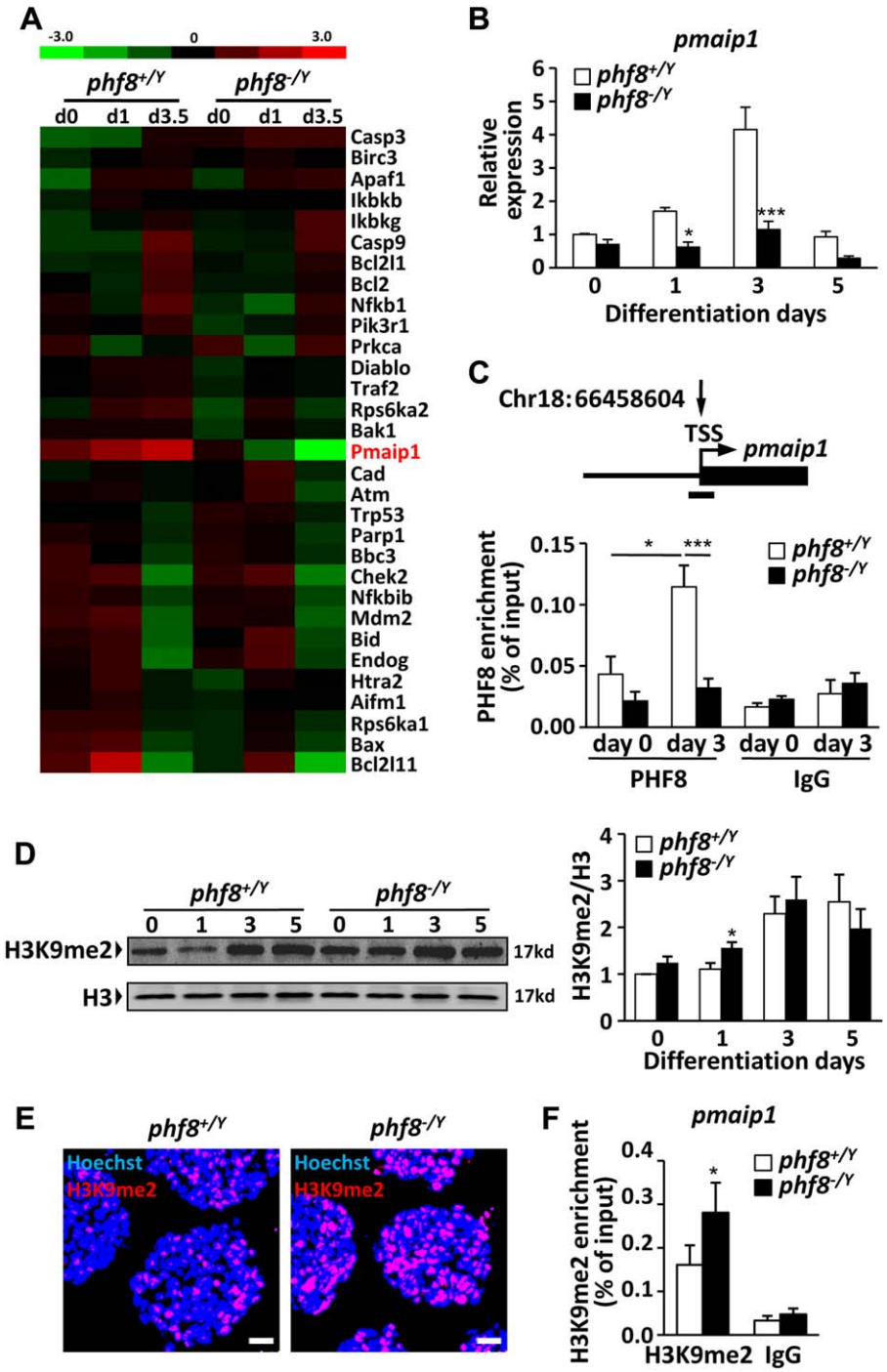

Figure 5. *pmaip1* is a direct target gene of plant homeo domain finger protein 8 (PHF8) in mouse embryonic stem cells (mESCs). (**A**): Microarray gene expression heat map depicting the expression of apoptosis-related genes at differentiation days 0, 1 and 3.5 in *phf8*$^{+/Y}$ and *phf8*$^{-/Y}$ ESCs. The expression values in log2 scale were calculated and presented on the heat map with red representing highly abundant transcripts and green representing poorly abundant transcripts. $n = 3$. (**B**): qRT-PCR analysis of *pmaip1* during the ESC differentiation. (**C**): ChIP assay of PHF8 around the TSS of *pmaip1* in *phf8*$^{+/Y}$ and *phf8*$^{-/Y}$ ESCs at differentiation days 0 and 3. $n = 4$ each. (**D**): Western blot analysis of H3K9me2 and H3 in *phf8*$^{+/Y}$ and *phf8*$^{-/Y}$ ESCs during the differentiation. H3 was used as a loading control. $n = 9$. (**E**): H3K9me2 staining in *phf8*$^{+/Y}$ and *phf8*$^{-/Y}$ embryoid bodies (EBs) at differentiation day 1. Scale bars = 25 μm. (**F**): ChIP assay of H3K9me2 around the TSS of *pmaip1* in *phf8*$^{+/Y}$ and *phf8*$^{-/Y}$ ESCs at differentiation day 3. $n = 4$. Data are presented as mean ± SEM. *, $p < .05$; **, $p < .01$; ***, $p < .001$ compared with the corresponding *phf8*$^{+/Y}$ value or d0.

an increase in cardiomyocyte progenitors and cardiomyocytes (Figs. 1C, 2C). Moreover, deletion of *phf8* specifically inhibits apoptosis of Flk-1^{+} mesodermal cells with a concomitant reduction in Annexin V^{+} staining (Fig. 4D) and cardiac differentiation (Fig. 2B--E), while the ratio of TUNEL^{+} to either NESTIN^{+} (ectodermal cells) or SOX17^{+} (endodermal cells) cells does not differ between the *phf8*$^{+/Y}$ and *phf8*$^{-/Y}$ lines (Supporting Information Fig. S3C, S3D). Consistently, the proportion of early apoptotic cells

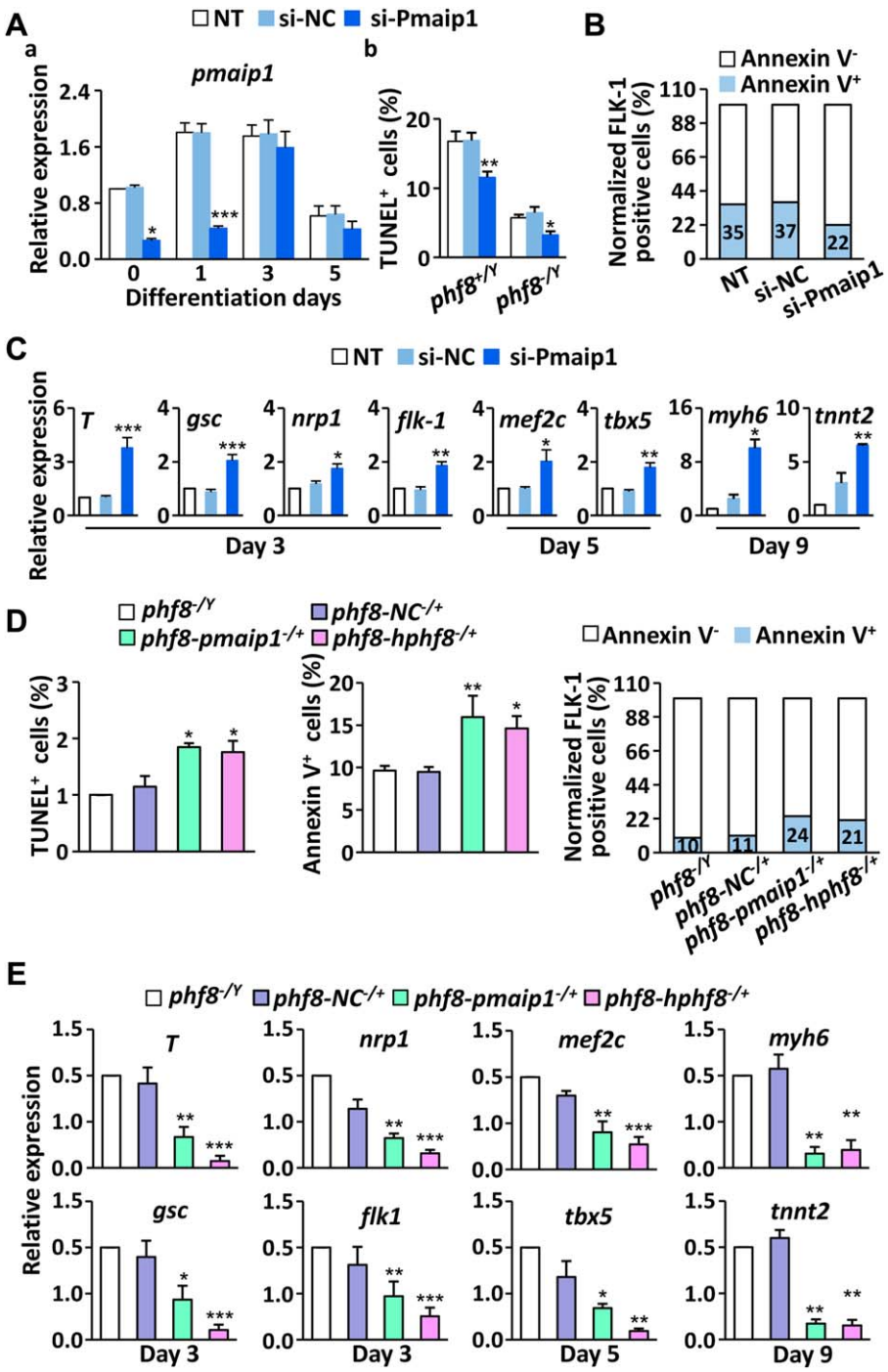

Figure 6. Plant homeo domain finger protein 8 (PHF8) regulates the mesodermal and cardiac differentiation through *pmaip1*. (**A-a**): qRT-PCR analysis of the *pmaip1* expression in *phf8*$^{+/Y}$ ESCs after being transiently transfected with si-NC or si-Pmaip1. $n = 4$. (A-**b**): Apoptosis cells were quantified by flow cytometry analysis of TUNEL assay at differentiation day 3 in *phf8*$^{+/Y}$ and *phf8*$^{-/Y}$ ESCs after transient transfection with si-NC or si-Pmaip1. $n = 3$. (**B**): Cells double stained with FLK-1 and Annexin V were analyzed by flow cytometry at differentiation day 4. $n = 4$. (**C**): qRT-PCR analysis of the expression of *T, gsc, flk-1, nrp1, tbx5, mef2c, myh6*, and *tnnt2* in *phf8*$^{+/Y}$ ESCs after transient transfection with si-NC or si-Pmaip1. $n = 5$. (**D**): Flow cytometry detection of TUNEL positive cells at differentiation day 3, Annexin V positive cells and double stained FLK-1 and Annexin V at differentiation day 4 in *phf8*$^{-/Y}$, *phf8-NC*$^{-/+}$, *phf8-pmaip1*$^{-/+}$, and *phf8-hPHF8*$^{-/+}$ mouse embryonic stem cells (mESCs). $n = 4$. (**E**): qRT-PCR analysis of the expression of *T, gsc, flk-1, nrp1, tbx5, mef2c, myh6*, and *tnnt2* in *phf8*$^{-/Y}$, *phf8-NC*$^{-/+}$, *phf8-pmaip1*$^{-/+}$, and *phf8-hPHF8*$^{-/+}$ mESCs. $n = 3$. Data are presented as mean ± SEM. *, $p < .05$; **, $p < .01$; ***, $p < .001$ compared with the corresponding *phf8*$^{+/Y}$ or *phf8*$^{-/Y}$ value.

(Annexin V$^+$) in *pmaip1*-knockdown (Fig. 6B) is also decreased, while *pmaip1*-overexpression or *hPHF8*-overexpression in *phf8*$^{-/Y}$ cells increase the proportion of TUNEL$^+$ and Annexin V$^+$ cells simultaneously with a reduction in mesodermal and cardiac differentiation (Fig. 6D, 6E). These findings indicate that the PHF8 functions, at least partially, through regulation of apoptosis.

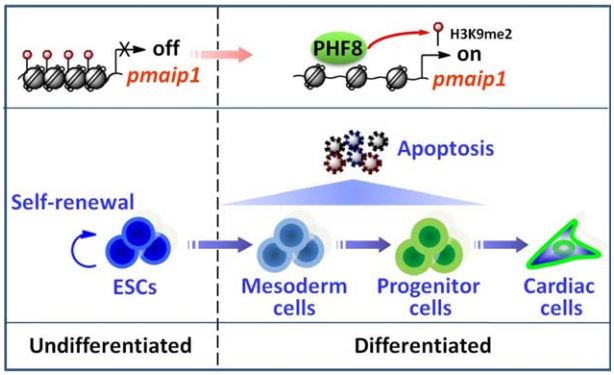

Figure 7. A proposed model for the regulation of *phf8* in ESC apoptosis and lineage commitment.

It is well known that the regulation of apoptosis is of critical importance for proper ESC differentiation and embryo development [8, 43]. ESC differentiation is regulated by apoptosis induced by MAPK activation [7] and IP_3R3-regulated Ca^{2+} release [5]. Previously only histone 3 lysine 4 methyltransferase MLL2 had been shown to activate the antiapoptotic gene *bcl2* to inhibit apoptosis during ESC differentiation [44]. The data presented, here, extends and reveals the importance of epigenetic controls in the activation of proapoptotic gene associated with ESC differentiation.

Mesodermal and cardiac differentiation have been shown to be regulated by the histone demethylase ubiquitously transcribed tetratricopeptide repeat, X chromosome (UTX) [13, 45] and jumonji domain–containing protein 3 (JMJD3) [12] through transcriptional activation of mesodermal and cardiac genes. These findings together with those presented in this paper support the critical role of histone demethylases in lineage commitment through regulatory mechanisms that control the expression of core lineage specific transcription factors and apoptotic genes. The decrease in apoptosis through deletion of *phf8* can be attributed to the maintenance of repressive H3K9me2 mark on the TSS of *pmaip1* after *phf8* deletion, resulting in a ~70% downregulation of *pmaip1* at differentiation day 3 in the $phf8^{-/Y}$ cells (Fig. 5B). The pro-apoptotic gene *pmaip1* is, therefore, epigenetically regulated by the histone demethylase, which subsequently affects the mesodermal and cardiac differentiation.

pmaip1 is a Bcl2 homology domain 3 (BH3)-only protein that acts as an important mediator of apoptosis [46]. Its expression is regulated transcriptionally by various transcription factors and, when present, it acts to promote cell death in a variety of ways [21] including caspase 3 dependent [47] and independent apoptosis [48] and autophagy [40]. Here, we find that PHF8 and its regulation on the *pmaip1* promote DNA fragmentation and cell death most likely through a caspase 3-independent pathway. This conclusion is based on the observation that neither the ratio of cleaved caspase 3 to total caspase 3 [49, 50] nor PARP1, a downstream target of caspase 3, is significantly affected. While this may be explained as the inhibitor of apoptosis proteins can counteract the function of caspase 3 [51, 52], the exact mechanisms we observed here need to be further explored.

Functionally, knockdown of *pmaip1* confers significant protection to apoptosis (Fig. 6B), while the increase in *pmaip1* occurs concomitantly with the enhancement in apoptosis observed during the early stage of cardiac differentiation (Fig. 4A--4C). The potential pmaip1-mediated apoptosis pathway might be explained by the following possibilities: (i) similar as BNIP3 (another BH3-only protein) which acts in the death of cardiac myocytes during exposure to hypoxia and acidosis without significant caspase activation [53], *pmaip1* might activate mitochondrial permeability transition pore but not mitochondrial apoptosis-inducing channel and causes the caspase 3-independent cell death [54]; and (ii) *pmaip1* would induce the direct DNA damage? which has been proved to mediate the cell death pathway involved in the reactive oxygen species generation in Soas-2 osteogenic sarcoma cells [55, 56]. Further studies are needed to elucidate the regulatory mechanisms of *pmaip1* on the caspase 3-independent cell death in differentiating ESCs.

Our findings appear to contradict publications reporting that PHF8 promotes neuronal differentiation of P19 cells [19]. Since the retinoic acid (RA) receptor was implicated in this process and our mesodermal induction system does not utilize RA [23], the differences are likely model system dependent, however, the role of RA requires further attention. Alternatively, function and expression of PHF8 may differ or be gene specific among cell types. In the undifferentiated state of mESC, PHF8 as well as histone H3K27 demethylases UTX [13, 45] and JMJD3 [12] are dispensable to ESC proliferation (Fig. 3D, 3E) and apoptosis (Fig. 4). PHF8, however, regulates the proliferation and apoptosis of self-renewing cancer cells. It is highly expressed in prostate cancer cells [57], Hela cells [58], esophageal squamous cell carcinoma [59], and human nonsmall cell lung cancer cells [60]. Knockdown of *phf8* in these cancerous cells results in a decrease of proliferation due to the poor cell cycle and the induction of apoptosis, while we show here that knockout of *phf8* does not affect proliferation or cell cycle in undifferentiated ESCs. These differences highlight the distinction in the function and regulation of PHF8 between potentially tumorigenic mESCs and cancer cells.

Conclusion

This study has identified a previously unrecognized function of histone demethylase PHF8 in the mesodermal and cardiac differentiation of ESCs through the control of apoptosis and the regulation of a proapoptotic gene. Mechanistically, PHF8 promotes apoptosis by removing the repressive H3K9me2 mark from the TSS of a pro-apoptotic gene *pmaip1*. Loss of this repressive mark permits or promotes *pmaip1* transcription, which promotes caspase 3-independent DNA fragmentation and cell death. Deletion of *phf8*, in contrast, represses *pmaip1* expression and reduces apoptosis in differentiating cells, which leads to augmented mesodermal lineage specification and cardiac cell commitment (Fig. 7) but not to the early ectodermal or endodermal differentiation. These results establish a new paradigm of the epigenetic control essential to the early ESC differentiation and lineage commitment through regulating apoptosis.

Acknowledgments

This study was supported by grants from the National Basic Research Program of China (2011CB965300; 2014CB965100), the Strategic Priority Research Program of CAS

(XDA01020204), the National Natural Science Foundation of China (31030050; 81520108004), and the National Science and Technology Major Project of China (2012ZX09501001) to H.T.Y. We thank Dr. Jiemin Wong for kindly providing the *hPHF8* plasmid.

Author Contributions

Y.T. and Y.-Z.H.: conception and design, collection and/or assembly of data, data analysis and interpretation and manuscript writing; H.J.B. and Q.W.: collection and/or assembly of data; C.C.: provision of study material; J.Y.L.: conception and design; K.R.B.: manuscript writing; H.T.Y.: conception and design, data analysis and interpretation, manuscript writing, financial support and final approval of manuscript. Y.T. and Y.Z.H. contributed equally to this article. Y.T. and Y.-Z.H contributed equally to this work.

Disclosure of Potential Conflicts of Interest

The authors indicate no potential conflicts of interest.

References

1 Evans MJ, Kaufman MH. Establishment in culture of pluripotential cells from mouse embryos. Nature 1981;292:154–156.
2 Keller G. Embryonic stem cell differentiation: Emergence of a new era in biology and medicine. Genes Dev 2005;19:1129–1155.
3 Duval D, Reinhardt B, Kedinger C et al. Role of suppressors of cytokine signaling (Socs) in leukemia inhibitory factor (LIF) - dependent embryonic stem cell survival. FASEB J 2000;14:1577–1584.
4 Duval D, Malaise M, Reinhardt B et al. A p38 inhibitor allows to dissociate differentiation and apoptotic processes triggered upon LIF withdrawal in mouse embryonic stem cells. Cell Death Differ 2004;11:331–341.
5 Liang J, Wang YJ, Tang Y et al. Type 3 inositol 1,4,5-trisphosphate receptor negatively regulates apoptosis during mouse embryonic stem cell differentiation. Cell Death Differ 2010;17:1141–1154.
6 Joza N, Susin SA, Daugas E et al. Essential role of the mitochondrial apoptosis-inducing factor in programmed cell death. Nature 2001;410:549–554.
7 Duval D, Trouillas M, Thibault C et al. Apoptosis and differentiation commitment: Novel insights revealed by gene profiling studies in mouse embryonic stem cells. Cell Death Differ 2006;13:564–575.
8 Fuchs Y, Steller H. Programmed cell death in animal development and disease. Cell 2011;147:742–758.
9 Gan Q, Yoshida T, McDonald OG et al. Concise review: Epigenetic mechanisms contribute to pluripotency and cell lineage determination of embryonic stem cells. Stem Cells 2007;25:2–9.
10 Adamo A, Sese B, Boue S et al. LSD1 regulates the balance between self-renewal and differentiation in human embryonic stem cells. Nat Cell Biol 2011;13:652–659.
11 Wang J, Park JW, Drissi H et al. Epigenetic regulation of miR-302 by JMJD1C inhibits neural differentiation of human embryonic stem cells. J Biol Chem 2013:289;2384–2395.
12 Ohtani K, Zhao C, Dobreva G et al. Jmjd3 controls mesodermal and cardiovascular differentiation of embryonic stem cells. Circ Res 2013:113;856–862.
13 Wang C, Lee JE, Cho YW et al. UTX regulates mesoderm differentiation of embryonic stem cells independent of H3K27 demethylase activity. Proc Natl Acad Sci USA 2012;109:15324–15329.
14 Feng WJ, Yonezawa M, Ye J et al. PHF8 activates transcription of rRNA genes through H3K4me3 binding and H3K9me1/2 demethylation. Nat Struct Mol Biol 2010;17:445–450.
15 Zhu Z, Wang Y, Li X et al. PHF8 is a histone H3K9me2 demethylase regulating rRNA synthesis. Cell Res 2010;20:794–801.
16 Laumonnier F, Holbert S, Ronce N et al. Mutations in PHF8 are associated with X linked mental retardation and cleft lip/cleft palate. J Med Genet 2005;42:780–786.
17 Abidi FE, Miano MG, Murray JC et al. A novel mutation in the PHF8 gene is associated with X-linked mental retardation with cleft lip/cleft palate. Clin Genet 2007;72:19–22.
18 Koivisto AM, Ala-Mello S, Lemmela S et al. Screening of mutations in the PHF8 gene and identification of a novel mutation in a Finnish family with XLMR and cleft lip/cleft palate. Clin Genet 2007;72:145–149.
19 Qiu J, Shi G, Jia Y et al. The X-linked mental retardation gene PHF8 is a histone demethylase involved in neuronal differentiation. Cell Res 2010;20:908–918.
20 Qi HH, Sarkissian M, Hu GQ et al. Histone H4K20/H3K9 demethylase PHF8 regulates zebrafish brain and craniofacial development. Nature 2010;466:503–507.
21 Ploner C, Kofler R, Villunger A. Noxa: At the tip of the balance between life and death. Oncogene 2008;27:S84–S92.
22 Yang HT, Tweedie D, Wang S et al. The ryanodine receptor modulates the spontaneous beating rate of cardiomyocytes during development. Proc Natl Acad Sci USA 2002;99:9225–9230.
23 Watanabe K, Kamiya D, Nishiyama A et al. Directed differentiation of telencephalic precursors from embryonic stem cells. Nat Neurosci 2005;8:288–296.
24 Mfopou JK, Geeraerts M, Dejene R et al. Efficient definitive endoderm induction from mouse embryonic stem cell adherent cultures: A rapid screening model for differentiation studies. Stem Cell Res 2014;12:166–177.
25 Cao N, Liu Z, Chen Z et al. Ascorbic acid enhances the cardiac differentiation of induced pluripotent stem cells through promoting the proliferation of cardiac progenitor cells. Cell Res 2012;22:219–236.
26 Tang Y, Chen ZY, Hong YZ et al. Expression profiles of histone lysine demethylases during cardiomyocyte differentiation of mouse embryonic stem cells. Acta Pharmacol Sin 2014;35:899–906.
27 Tusher VG, Tibshirani R, Chu G. Significance analysis of microarrays applied to the ionizing radiation response. Proc Natl Acad Sci USA 2001;98:5116–5121.
28 Bernemann C, Greber B, Ko K et al. Distinct developmental ground states of epiblast stem cell lines determine different pluripotency features. Stem Cells 2011;29:1496–1503.
29 Russ AP, Wattler S, Colledge WH et al. Eomesodermin is required for mouse trophoblast development and mesoderm formation. Nature 2000;404:95–99.
30 van den Ameele J, Tiberi L, Bondue A et al. Eomesodermin induces Mesp1 expression and cardiac differentiation from embryonic stem cells in the absence of Activin. EMBO Rep 2012;13:355–362.
31 Yang L, Soonpaa MH, Adler ED et al. Human cardiovascular progenitor cells develop from a KDR + embryonic-stem-cell-derived population. Nature 2008;453:524–528.
32 Kattman SJ, Huber TL, Keller GM. Multipotent flk-1 + cardiovascular progenitor cells give rise to the cardiomyocyte, endothelial, and vascular smooth muscle lineages. Dev Cell 2006;11:723–732.
33 Fantin A, Herzog B, Mahmoud M et al. Neuropilin 1 (NRP1) hypomorphism combined with defective VEGF-A binding reveals novel roles for NRP1 in developmental and pathological angiogenesis. Development 2014;141:556–562.
34 Nelson TJ, Faustino RS, Chiriac A et al. CXCR4+/FLK-1 + biomarkers select a cardiopoietic lineage from embryonic stem cells. Stem Cells 2008;26:1464–1473.
35 Riley P, Anson-Cartwright L, Cross JC. The Hand1 bHLH transcription factor is essential for placentation and cardiac morphogenesis. Nat Genet 1998;18:271–275.
36 Hiroi Y, Kudoh S, Monzen K et al. Tbx5 associates with Nkx2-5 and synergistically promotes cardiomyocyte differentiation. Nat Genet 2001;28:276–280.
37 Magli A, Schnettler E, Swanson SA et al. Pax3 and Tbx5 specify whether PDGFRalpha + cells assume skeletal or cardiac muscle fate in differentiating embryonic stem cells. Stem Cells 2014;32:2072–2083.
38 Ricci JE, Gottlieb RA, Green DR. Caspase-mediated loss of mitochondrial function and generation of reactive oxygen species during apoptosis. J Cell Biol 2003;160:65–75.
39 Duriez PJ, Shah GM. Cleavage of poly(-ADP-ribose) polymerase: A sensitive parameter to study cell death. Biochem Cell Biol 1997;75:337–349.
40 Elgendy M, Sheridan C, Brumatti G et al. Oncogenic Ras-induced expression of Noxa and Beclin-1 promotes autophagic cell death

and limits clonogenic survival. Mol Cell 2011; 42:23–35.
41 Wensveen FM, Geest CR, Libregts SF et al. BH3-only protein Noxa contributes to apoptotic control of stress-erythropoiesis. Apoptosis 2013;18:1306–1318.
42 Zhong JX, Zhou L, Li Z et al. Zebrafish Noxa promotes mitosis in early embryonic development and regulates apoptosis in subsequent embryogenesis. Cell Death Differ 2014;21:1013–1024.
43 Cheung H-H, Liu X, Rennert OM. Apoptosis: Reprogramming and the fate of mature cells. ISRN Cell Biol 2012;2012:1–8.
44 Lubitz S, Glaser S, Schaft J et al. Increased apoptosis and skewed differentiation in mouse embryonic stem cells lacking the histone methyltransferase Mll2. Mol Biol Cell 2007;18:2356–2366.
45 Lee S, Lee JW, Lee SK. UTX, a histone H3-lysine 27 demethylase, acts as a critical switch to activate the cardiac developmental program. Dev Cell 2012;22:25–37.
46 Oda E, Ohki R, Murasawa H et al. Noxa, a BH3-only member of the Bcl-2 family and candidate mediator of p53-induced apoptosis. Science 2000;288:1053–1058.
47 Qing G, Li B, Vu A et al. ATF4 regulates MYC-mediated neuroblastoma cell death upon glutamine deprivation. Cancer Cell 2012;22:631–644.
48 Hu W, Ge Y, Ojcius DM et al. p53 signalling controls cell cycle arrest and caspase-independent apoptosis in macrophages infected with pathogenic Leptospira species. Cellular Microbiol 2013:15;1642–1659.
49 Freeman-Anderson NE, Pickle TG, Netherland CD et al. Cannabinoid (CB2) receptor deficiency reduces the susceptibility of macrophages to oxidized LDL/oxysterol-induced apoptosis. J Lipid Res 2008;49:2338–2346.
50 Wu Y, Song W. Regulation of RCAN1 translation and its role in oxidative stress-induced apoptosis. FASEB J 2013;27:208–221.
51 Deveraux QL, Roy N, Stennicke HR et al. IAPs block apoptotic events induced by caspase-8 and cytochrome c by direct inhibition of distinct caspases. EMBO J 1998;17: 2215–2223.
52 Bratton SB, Lewis J, Butterworth M et al. XIAP inhibition of caspase-3 preserves its association with the Apaf-1 apoptosome and prevents CD95- and Bax-induced apoptosis. Cell Death Differ 2002;9:881–892.
53 Kubasiak LA, Hernandez OM, Bishopric NH et al. Hypoxia and acidosis activate cardiac myocyte death through the Bcl-2 family protein BNIP3. Proc Natl Acad Sci USA 2002; 99:12825–12830.
54 Webster KA, Graham RM, Thompson JW et al. Redox stress and the contributions of BH3-only proteins to infarction. Antioxid Redox Signal 2006;8:1667–1676.
55 Ray R, Chen G, Vande Velde C et al. BNIP3 heterodimerizes with Bcl-2/Bcl-X(L) and induces cell death independent of a Bcl-2 homology 3 (BH3) domain at both mitochondrial and nonmitochondrial sites. J Biol Chem 2000;275:1439–1448.
56 Vande Velde C, Cizeau J, Dubik D et al. BNIP3 and genetic control of necrosis-like cell death through the mitochondrial permeability transition pore. Mol Cell Biol 2000;20: 5454–5468.
57 Bjorkman M, Ostling P, Harma V et al. Systematic knockdown of epigenetic enzymes identifies a novel histone demethylase PHF8 overexpressed in prostate cancer with an impact on cell proliferation, migration and invasion. Oncogene 2011;31:3444–3456.
58 Liu W, Tanasa B, Tyurina OV et al. PHF8 mediates histone H4 lysine 20 demethylation events involved in cell cycle progression. Nature 2010;466:508–512.
59 Sun X, Qiu JJ, Zhu S et al. Oncogenic features of PHF8 histone demethylase in esophageal squamous cell carcinoma. PLoS One 2013;8:e77353.
60 Shen Y, Pan X, Zhao H. The histone demethylase PHF8 is an oncogenic protein in human non-small cell lung cancer. Biochem Biophys Res Commun 2014;451:119–125.


See www.StemCells.com for supporting information available online.

